J Mater Sci (2007) 42:2037–2047
DOI 10.1007/s10853-006-0776-2

Processing and properties of titanium–titanium boride (TiB_w) matrix composites—a review

K. Morsi · V. V. Patel

Received: 12 February 2006 / Accepted: 8 August 2006 / Published online: 1 February 2007

Abstract Although titanium (Ti) alloys possess desirable properties such as specific strength, corrosion resistance and low density, their low specific stiffness and wear resistance have restricted their widespread application. Recently, composite strategies have provided means for overcoming these limitations. Titanium boride (TiB_w) in-situ whisker reinforcements are currently recognized as one of the most compatible and effective reinforcements for Ti. This paper provides an overview of recent activities in this evolving area of Ti–TiB composites, covering processing, properties and potential applications.

Introduction

The interest in titanium matrix composites (TMCs) has grown significantly over the past few years. This has been brought about by their unique properties which include high specific strength, specific stiffness and specific fatigue resistance (high cycle fatigue) [1]. A number of reinforcements have been suggested/used including Ti_5Si_3, CrB, B_4C and SiC [2] and TiC [3]. The reinforcements usually need to be stiffer than the matrix, have a similar thermal expansion coefficient to the matrix and to be also chemically stable. Recently TiB has been identified as probably the most suitable discontinuous reinforcement for the Ti system (Fig. 1), which is both thermodynamically & mechanically stable (generating minimal residual stresses). TiB single crystal whiskers have recently been generated in Ti matrices via cost-effective in-situ processing [4], and have been known to bond very well to the Ti matrix and generate very clean interfaces [5]. Hence the interest in these materials has been growing over the past few years. Figure 2 shows the number of cumulative journal publications per year dealing with Ti–TiB composites from 1984 to 2005 inclusive, as an example.

Although some of these composites have been produced through techniques such as casting and ingot metallurgy [6], the majority of this published work has focused on the powder metallurgy (PM) or powder-based route (Fig. 3), largely due to its ability for microstructural control, near net shape processing and minimal material waste.

Two of the current obstacles facing titanium metal matrix composites are their high cost and low fracture toughness and ductility (at high reinforcement volume fractions) [7]. These however can be tackled by the use of net shape processing, reduced raw material cost, low-energy processing approaches and microstructural design. A number of recent manufacturing techniques based on powder metallurgy processing including the *Blended Elemental P/M method* have made breakthroughs with respect to producing titanium composites cost effectively, such that they are now used as exhaust valves in Toyota automotive engines [8]. Abkowitz et al. [9] and Froes et al. [10], recently discussed the applications of discontinuously reinforced titanium composites. The following is a summary of some of the applications/potential applications for Ti matrix composites as reported to-date:

K. Morsi (✉) · V. V. Patel
Department of Mechanical Engineering, San Diego State University, 5500 Campanile Drive, San Diego, CA 92182, USA
e-mail: kmorsi@mail.sdsu.edu

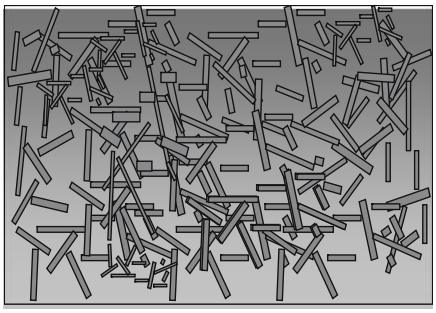

Fig. 1 Schematic of TiB whiskers in a Ti matrix

- Manufacturing: Die casting shot sleeve liners.
- Military: Tank track and wheeled vehicle undercarriage components.
- Automotive: Valves, connecting rods and piston pins
- Biomedical: Spinal articulating devices
- Sporting Goods: hockey skate blades, knives

Application expectations for titanium metal matrix composites include missile fins, domed rocket cases and aircraft engine components [11]. TiB reinforcements have also been used in functionally graded materials [12], and in the production of hybrid composites with other reinforcements such as TiC [13] and Y_20_3 [14].

Although great advancements have been made in terms of improved stiffness, wear resistance and room/high temperature strengths of TiB reinforced titanium composites, this has been at the expense of ductility and toughness (a compromise that has plagued composite development). This paper provides an overview of the recent activities and current understanding of Ti–TiB processing and properties, an area that is rapidly growing.

TiB in-situ reinforcements

In-situ reinforcements for metal matrix composites have been under investigation for some time. Recently, Tjong and Ma [15] reviewed the microstructural and mechanical characteristics of in-situ metal matrix composites. Combined in-situ formation and thermo-mechanical processing has also been studied for other reinforced and un-reinforced systems by one of the authors [16–18]. One of the difficulties previously encountered in reinforcing Ti has been to find a reinforcement material that is both chemically and mechanically stable. For example although SiC continuous filaments have been successfully used for reinforcing titanium, it is usually achieved via the presence of a pyrocarbon sacrificial layer, as SiC is known to react with the Ti matrix [19]. The in-situ reinforcement of Ti has therefore been under recent intense investigation, as part of the constant search for more effective & compatible reinforcements for Ti.

There are a number of advantages to in-situ formation of whisker reinforcements in general, these include:

1. Safety: having to deal with whiskers during processing is known to be a health hazard as they can lodge in the lungs.
2. Some reinforcements such as TiB have been difficult to produce in single crystal whisker form, since they form through a peritectic reaction (titanium rich liquid + TiB_2 $\rightarrow$ TiB) [4] in the Ti–B system at this composition (Fig. 4).
3. The cost of whiskers and their processing is usually high, and in-situ processing may represent a cost effective alternative.

As previously mentioned TiB whiskers formed through in-situ reactions have been reported to bond very well with the Ti matrix and generate very clean interfaces [5]. The chemical stability of the TiB-Ti interface is due to the absence of intermediate phases between TiB and Ti, as can be seen in the Ti–B phase diagram (Fig. 4). Moreover, TiB whiskers are much stiffer (E = 371 GPa [21], other values for the elastic modulus of TiB have also been reported such as E = 550 GPa [22] (here the authors assumed TiB to

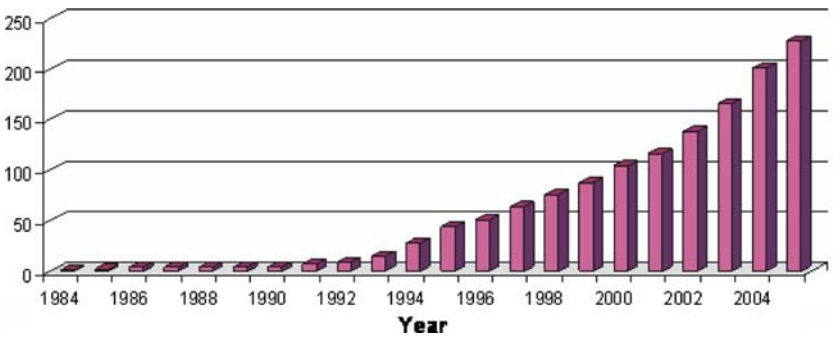

Fig. 2 Number of cumulative journal publications per year dealing with Ti–TiB composites (Data for 1984–2005 inclusive, Source: Ei-compendex)

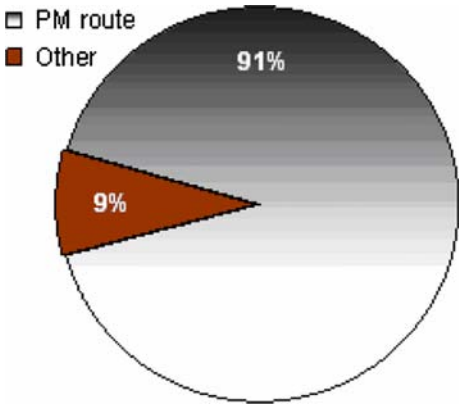

Fig. 3 Percentage of papers using powders (powder metallurgy) as a means of processing (Data for 1984–2005 inclusive, Source: Ei-compendex)

have the same Young's modulus as TiB_2, which may not be true)) than Ti (E = 110 GPa), and at the same time the coefficient of thermal expansion (CTE) of both materials are close ($CTE_{Ti} = 9.0 \times 10^{-6}$ K^{-1}, $CTE_{TiB} = 8.6 \times 10^{-6}$ K^{-1} [2]). This has the effect of minimizing the residual stresses in the final composite. It is also interesting to note that TiB and Ti have almost equal densities (ρ_{Ti} = 4.57 g cm^{-3}, ρ_{TiB} = 4.56 g cm^{-3} [4]).

The TiB and TiB_2 phases have B27 and C32 crystal structures respectively [23]. It has been reported that TiB whisker growth occurs along the [010] direction (i.e. one dimensional), while that of the TiB_2 is two-dimensional along the $<1\bar{1}00>$ directions [23], and hence a whisker morphology is generated in the former.

The boron source needed to generate TiB can either come in the form of TiB_2, B, CrB, MoB or other compounds that contain both α and/or β-Ti stabilizers. The matrix alloying elements can even be added separately in the form of compounds, for example vanadium aluminide (VAl) can be used, which can sometimes even be effective way of reducing the cost of the raw materials [8]. The state of the initial Ti alloying elements can also have an influence on the process. For example, recently Li et al. [24] carried out differential thermal analysis (DTA) experiments on Ti/B/Al powder mixtures, and concluded that Al additions can aid the formation of TiB whiskers when Al is in the molten state by providing a medium for fast diffusion of Ti & B. The results are applicable to the production of TiB-reinforced titanium composites via reactive sintering. Fan et al. [22] formed Ti–TiB composites with varying TiB volume fractions by consolidation of rapidly solidified Ti-6Al-4V alloy powders with different levels of boron addition. They found that the formation of even 0.1 volume fraction of TiB can yield approximately a 20% increase in the Young's modulus of Ti. According to Gorsse et al. [2] an aspect ratio greater than 10 and more than 0.1 volume fraction of TiB whiskers are needed in order to effectively reinforce titanium. By forming 0.2 volume fraction of TiB, they have managed to increase the Ti Young's modulus by ~45%. The study also concluded that TiB is the best overall reinforcement for Ti out of Ti_5Si_3, CrB, B_4C and SiC, generating minimal residual stresses, having a higher stiffness (similar to CrB) and

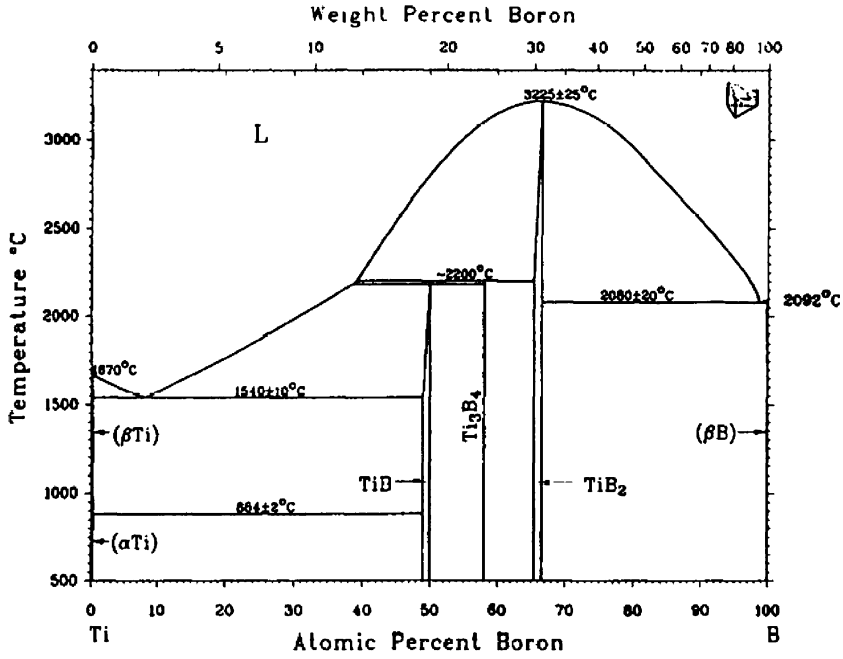

Fig. 4 The Ti–B phase diagram-showing the absence of any intermediate phase between TiB & Ti. [20]

better chemical stability. Aligned TiB whiskers (with aspect ratios ranging from 4 to 40) have also been processed using reactive hot pressing followed by hot extrusion, using different starter powder mixtures including Ti–B, Ti–TiB_2, Ti–B_4C and Ti–BN [5].

The in-situ formation of TiB within the titanium matrix can be accomplished through the following reaction:

$$Ti + TiB_2 \rightarrow 2TiB \quad (1)$$

It has been reported that although this reaction has a slightly negative Gibb's free energy of formation, compared with other reactions that appear more favorable, in general TiB whiskers will always be favored to form as long as the overall boron average content in the reaction zone is below 18 wt.% (or in other words there is excess Ti [25]), and that enough time is available for diffusion [26].

Processing of Ti–TiB composites

Ti–TiB composites with varying volume fractions and TiB morphologies have been processed using a number of approaches. In cases it has even been reported that the volume fraction of the elemental boron source can have an influence on the final TiB morphology.

Radhakrishna Bhat et al. [27] examined the reaction hot pressing of Ti–TiB composites and generated surprisingly rounded TiB morphologies at 0.67 TiB volume fraction. Sahay et al. [28], examined the effect of TiB volume fraction on the resulting TiB morphology, they found that at low TiB volume fractions, long needle-like TiB was generated which were randomly oriented, at intermediate-to-high volume fractions (0.55, 0.73 & 0.86) colonies of fine and well packed TiB were generated while at the highest volume fraction (0.92) elongated and coarse TiB particles were formed with few whiskers observed. It was also noted that for the highest TiB volume fractions (0.86 & 0.92) residual TiB_2 was also present.

Also in another study by Panda and Ravi Chandran [26] (in which they included β-Ti stabilizing elemental powders), at high TiB_2 volume fraction, the TiB whiskers were found to cluster to again produce some sort of monolithic form. This has been explained by the lack of direct contact between all TiB_2 particles and Ti. In that case, if all the TiB_2 are not in intimate contact with Ti, and with the difficulty of diffusing Ti through TiB in order to reach the TiB_2 to continue the reaction, then TiB whiskers, TiB clusters and some remaining unreacted TiB_2 will be present in the final microstructure. This will therefore pose a problem when using a high volume fraction of TiB_2, i.e. for highly intended TiB volume fractions. Panda et al. in the same study also showed that on the other hand when a tri-modal powder particle size is used and the TiB_2 particles are in contact with Ti, only whiskers are generated, with no reaction products (namely Ti_3B_4). They used β-Ti stabilizing elemental particles of a particular size to just fill the interstitial sites between the Ti particles. In these experiments XRD was also used to identify phases, and therefore if Ti_3B_4 was present in amounts less than a few vol. % it could not be confirmed, however it was suggested that at least an almost complete reaction can be claimed [26]. Following this work, if TiB_2 with a bi-modal particle size distribution can be used at high reinforcement volume fractions it may also be possible to avoid clustered TiB and un-reacted TiB_2. Figure 5 illustrates this point for Ti–TiB_2 starting powder compacts (the figure has largely been adapted from reference 26 with some slight alterations, such as the absence of any β-Ti stabilizing elements; for the original figure relating to Ti–TiB_2 and β-Ti stabilizers, readers are suggested to refer to reference [26]). In a separate study, Feng et al. [29] also reported no reaction products at the interface between TiB and Ti when starting with Ti, FeMo and B powders. This may be due to the excess titanium present in the system, as previously mentioned. Xinghong et al. [30] reported similar results, where TiB_2 (an intermediate phase generated during the B + Ti reaction) remained in the final product at high volume fractions of TiB in Ti formed through self-propagating high temperature synthesis (SHS). They attributed this again to in-homogenous mixing and limited time for TiB_2 to transform to TiB (through the reaction $Ti + TiB_2 \rightarrow TiB$), owing to fast reaction times and cooling rates often experienced in SHS processing.

Although the work reported to date has contributed to our current understanding of the processing of Ti–TiB, the powder design may potentially have a significant influence on the developed morphology of the TiB whiskers and needs to be examined in detail. For example, the lack of TiB_2-Ti contact at high TiB_2 volume fractions can be overcome by *embedding* the TiB_2 particles in the titanium particles, to generate homogenously distributed TiB_2 within a continuous Ti matrix, where the TiB_2 particles will always be surrounded by Ti. This could be easily carried out through the process of mechanical alloying (MA). One possible advantage of using MA is the generation of defect structures within the Ti–TiB_2 composite particles which should provide improved diffusion characteristics during high temperature processing. The authors believe that another possibility is the

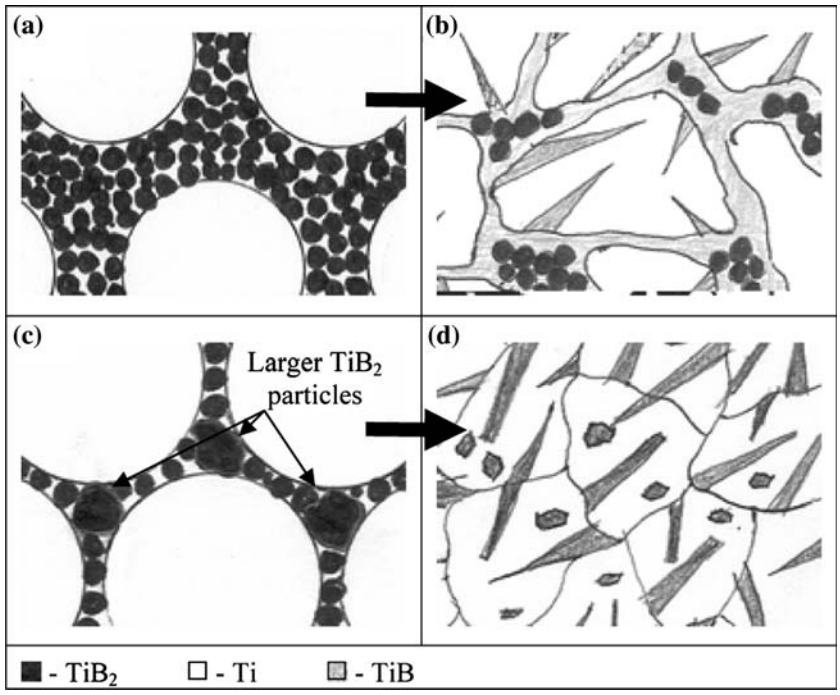

Fig. 5 The dependence of TiB morphology on elemental powder distribution (largely adapted from reference [26], with some slight alterations)

generation of Ti–TiB composite *powders* which can either be produced through the MA process under certain conditions or by heat treating the Ti–TiB_2 composites powders. After processing, the mechanically alloyed Ti–TiB_2 composite particles should have a homogenous distribution of TiB_2 or TiB within Ti.

MA was very recently conducted on mixtures of Ti, TiB_2 and FeMo (β-Ti stabilisers) for 10 hours in a planetary ball mill using a BPR of 10:1 [31]. The researchers were successful in generating composite powders and effectively dispersing the TiB_2 in Ti, and generating 0.1 TiB volume fraction in the titanium matrix after spark plasma sintering. They also reported the generation of defect structures in the milled powders which facilitated faster diffusion during the high temperature sintering process. In a separate publication up to 0.2 TiB volume fraction was formed from mechanically alloyed mixtures of with B, Ti and FeMo (β-Ti stabilisers) followed by vacuum hot pressing with no reported by-products at the interfaces after high temperature consolidation [29]. It is also important to point out that after the MA stage no actual alloying took place, but rather intimate mixing and composite particles consisting of the elemental constituents were generated, under the investigated milling conditions. To the best of the authors' knowledge no work has been reported on the generation of higher volume fraction of TiB-Ti composites by MA which presents an opportunity to examine the possibility of forming whiskers at high volume fraction rather than the reported clustered/rounded particles of TiB that often occur at high TiB volume fractions (as discussed earlier). It is important to maintain the whisker morphology for improved performance at high volume TiB fractions. The particle and microstructural evolution at considerably higher volume % TiB_2 may certainly have implications as to the composite particle matrix grain size and defect structures generated.

Reactive Hot Pressing [32], Reactive Pseudo Hot Isostatic Pressing [32], Spark Plasma Sintering [31] and Hot Extrusion [33] are some of the techniques used to process Ti–TiB composites. In most cases during high-temperature consolidation, simultaneous densification and formation of TiB occurs. Processes such as hot extrusion have the ability to align TiB whiskers [33]. The growth of TiB whiskers is one-dimensional as mentioned earlier and its kinetics depends strongly on temperature. Recent studies have suggested a parabolic growth of TiB in a titanium matrix, according to the following equations [23, 26]:

$$x = k\sqrt{t} \tag{2}$$

$$k = k_o \exp\left(\frac{-Q_k}{2RT}\right) \tag{3}$$

x is length of the whiskers, k is the temperature dependent growth rate, t is time at the processing temperature, k_o and Q_k are the frequency factor & activation energy for TiB growth respectively (reported to be 17.07×10^{-4} m/s$^{1/2}$ and 190.3 kJ/mol respectively [23]), R is the gas constant and T is the

temperature in Kelvin. The above equations have been used to obtain size estimates for TiB whiskers at varying temperatures [26].

On the other hand, recently Feng et al. [29], reported that TiB generated at grain boundaries were coarser than those generated within grains owing to faster grain boundary diffusion. Hence it may be possible to use the different activation energies and diffusion data to estimate the TiB whisker size at grain boundaries as opposed to that within the interior of the grains. In another study by Sahay et al. [28] a mechanism was put forward for the generation of multiple short TiB whiskers from one parent TiB_2 particle, which have sometimes been observed.

A recent interesting study that used the Ti + CrB → Cr + TiB reaction to generate Ti–TiB composites noted that in the initial stages TiB forms with a morphology of granular particles, however, if left for long enough time at the sintering temperature, the TiB granular particles were found to self divide into plate-like TiB particles [34]. The reasoning behind this phenomenon was attributed to the difference in the total interfacial energy between the two forms, which acted as a driving force for the division.

Combustion synthesis has been applied to the production of Ti–TiB, where the chemical energy generated during the reaction of elemental powders is utilized to form materials at low energies. One of the authors recently reviewed the combustion synthesis of Ni–Al materials [35]. In general, two modes of ignitions are usually used, one is SHS, as mentioned previously, where the powder compact is locally ignited at one region and a self-propagating reaction wave spreads throughout the remainder of the compact consuming the reactants and converting them into the intended product. The other mode is thermal explosion or volumetric combustion, where the whole volume of the compact is heated to the ignition temperature. Combustion synthesis reactions are known for their high exothermic nature, this is especially true when synthesizing Ti–TiB where the boron source is pure boron and therefore very high temperatures (termed combustion temperatures) are generated during the reaction [30]. These reactions have been reported to start when the compact temperature reaches the α/β Ti transition temperature (1155 K) [32]. It was found that as the amount of Ti is increased in the (Ti + B) mixture both the combustion temperature, wave velocity and resulting TiB size decrease [30]. This is because the excess Ti will not contribute in the reaction but rather act as a heat sink and would essentially buffer the reaction. High-density products were generated when the Ti was in the molten state during the reaction which facilitated pore filling. An optimum Ti content was reported for the particle size and experimental conditions used [30]. When the exothermic heat of formation generated from the elemental species is low, the thermal explosion or volumetric combustion mode of ignition is usually used. In a recent study, Kobayashi et al. [36] investigated the in-situ synthesis of Ti–TiB composites (at 1473 K for two hours under vacuum) of mechanically milled powder compacts of Ti-6Al-4V + TiB_2, Ti-6Al-4V + CrB, Ti-6Al-4V + MoB. The addition of reinforcements was found to significantly decrease the density of the final composites. This was more significant at the lowest reinforcement volume fractions for TiB_2 than for MoB. It is however noted that the reinforcements initial particle size were different (1.5 μm for TiB, 3.9 μm for MoB and 8.9 μm for CrB), and also there was no mention of the final particle size/particle size distribution after mechanical milling, both of which are parameters that can affect the final density of the composite. However when the material was followed by hot isostatic pressing (HIP) densities greater than 98% where achieve for all reinforcements and volume fractions. In the same work hot rolling was found to refine the TiB reinforcements and slightly align them. Also recently, Banerjee et al. [37] using a laser engineered net-shaping (LENS^{TM}) process on a powder feed of Ti and boron, generated Ti–TiB composites. However, nanometer scale TiB was observed and attributed to the solid state decomposition of boron supersaturated Ti-base matrix. In a separate study nanometric TiB whiskers have also been observed together with larger whiskers [26], which are expected to have a significant effect on the reported mechanical properties, and should be taken into account.

Once the material has been processed, the product is usually characterized by XRD and electron microscopy (scanning and transmission). Deep etching in Kroll's reagent is typically used prior to microstructural characterization. For volume fraction estimation, Panda et al. [26] used the direct comparison X-ray method [38], in which integrated intensities of the phase are computed assuming Gaussian distribution. The volume fractions were then calculated according to the following equation [26]:

$$V_{f,TiB} = \frac{R_{Ti} I_{TiB}}{R_{Ti} I_{TiB} + R_{TiB} I_{Ti}} \quad (4)$$

Where, I is the (hkl) peak integrated intensity, and R is an angular-dependent term. The procedure is described in detail for TiB volume fraction determination

in reference [26]. It is useful when difficulties arise in identifying all the TiB microscopically.

Mechanical properties of Ti–TiB composites

One of the advantages of TiB as reinforcement for Ti, is its higher elastic modulus, which has been usually estimated indirectly using the Tsai–Halpin equation [21, 39] for randomly oriented short fiber composites, where:

$$E_{\text{random}} = \frac{3}{8}E_{11} + \frac{5}{8}E_{22} \tag{5}$$

Where,

$$E_{11} = \frac{1 + 2\left(\frac{l_f}{d_f}\right)\eta_L V_f}{1 - \eta_L V_f} E_m, \tag{6}$$

$$E_{22} = \frac{1 + 2\eta_T V_f}{1 - \eta_T V_f} E_m, \tag{7}$$

$$\eta_T = \frac{\left(\frac{E_f}{E_m}\right) - 1}{\left(\frac{E_f}{E_m}\right) + 2} \tag{8}$$

&

$$\eta_L = \frac{\left(\frac{E_f}{E_m}\right) - 1}{\left(\frac{E_f}{E_m}\right) + 2\left(\frac{l_f}{d_f}\right)} \tag{9}$$

V_f and V_m = volume fraction of fiber and matrix.

E_m and E_f = elastic moduli of the matrix and fiber respectively.

E_{11} & E_{22} = Longitudinal and transverse moduli for short fiber composite (unidirectional) respectively.

$\frac{l_f}{d_f}$ = fiber aspect ratio

As previously mentioned, Fan et al. [40] found that the addition of even 0.1 volume fraction of TiB can yield approximately a 20% increase in the Young's modulus of Ti. Gorsse et al. [2] reported an increase of ~45% in the elastic modulus with 0.2 TiB volume fraction. The alignment of whiskers can also influence the Young's modulus. In a recent study [33], the Young's modulus of Ti–TiB composites with aligned TiB whiskers in the extrusion direction was reported to be 169 GPa compared with 159 GPa for randomly oriented TiB of the same 0.2 TiB volume fraction. At 0.4 TiB volume fraction, the Young's modulus was 205 GPa in the extrusion direction and 188 GPa in the transverse direction. Although not reported here, but one would expect a Young's modulus of greater than the 188 GPa (transverse direction) for the randomly oriented 0.4 TiB configuration. At the 0.4 TiB volume fraction the modulus values are approaching those of steel, as certainly one of the reported values suggests in Table 1. It may seem academic that to further gain increases in Young's modulus we simply keep increasing the TiB content. This however will come at the expense of ductility and fracture toughness. Attempts to resolve the problem of loss of ductility with increase in TiB volume fraction were carried out via the addition of β-Ti stabilizers, in order to generate a more ductile matrix [26]. In that study, the authors report a best value of 1.7% ductility for Ti–TiB composite with a 0.34 TiB volume fraction. However, this composite did not contain well-dispersed whiskers as the major TiB morphology but rather globular TiB clusters. This was however an improvement on a previously reported ductility close to zero for 0.30 TiB volume fraction [26, 47].

The addition of TiB has also been shown to increase the creep resistance of titanium [11, 43]. Tensile strength, fatigue strength and wear resistance have also been reported to increase with increase in TiB volume fraction [48]. Recently Li et al. [49], studied the in-situ crack nucleation and growth of Ti - TiB_w, and showed that crack bridging/pullout of the TiB whiskers and crack deflection are present as toughening mechanisms in these composites (Fig. 6). This study was conducted on a 0.1 TiB volume fraction composite. In another study using spark plasma sintering of Ti–FeMo–B, fracture toughness was found to generally decrease with increase in volume fraction (0.05–0.2) of TiB [7]. While the presence of reinforcements that promote toughening mechanisms in a composite is of benefit, the toughness of the matrix is also an important contributing factor. As more brittle reinforcements are added they replace tougher matrix material, and hence it is not surprising that the fracture toughness deceases with increase in TiB volume fraction beyond a certain TiB volume fraction. Super-plasticity was also recently confirmed for Ti–TiB composites [36]. Ravi Chandran and Panda [46] recently presented a summary of mechanical properties of Ti–TiB composites from 0.1–0.4 TiB volume fraction additions. Table 1 complied by the present authors is a significant expansion on

Table 1 Summary of some of the reported Mechanical Properties of TiB reinforced titanium alloys (the table is an expansion on a previously reported table [49], the current table covers reported work from 0.039 to 1.0 TiB volume fractions and also incorporates fracture toughness reported data)

TiB vol. %	Boron Source	Matrix	Process	Properties							Comments	Ref.
				VHN (or HRA)	Yield Strength (MPa)	UTS (MPa)	Ductility %	Young's Modulus (GPa)	Flexural Strength (MPa)	K_{1C} (MPa.m$^{1/2}$)		
0	–	Ti-6Al-4V	C+E+H	–	986	1035	–	110	–	39.9	–	41
0	–	Ti-22Al-27Nb	PM+HR+H	–	701	848	6.8	–	–	–	–	42
0	–	Ti	VAR+HS	–	164	179	20.7	109	–	–	–	43
3.1	B	Ti-6Al-4V	C+E+H	–	1041	1156	–	129	–	44	–	41
3.9	TiB_2	Ti-6Al-4V	RS+HIP	453	–	–	–	123.5	–	–	–	44
3.9	TiB_2	Ti-6Al-4V	RS+H+ HIP+F	526	–	–	–	130	–	–	–	44
5	TiB_2	Ti-6Al-4V	CS+HIP	~440	–	–	–	–	–	–	Ti added to matrix	36
5	MoB	Ti-6Al-4V	CS+HIP	~405	–	–	–	–	–	–	Mo added to matrix	36
5	CrB	Ti-6Al-4V	CS+HIP	~350	–	–	–	–	–	–	Cr added to matrix	36
5	B	Ti	VAR (MACS) +HS	–	639	787	12.5	121	–	–	–	43
5	B	Ti-4.0Fe-7.3Mo	SPS	–	–	–	–	~132	~1284	~9.7	Density ~100%	7
6.5	B	Ti-22Al-27Nb	IM+HR+H	–	818	992	4.0	–	–	–	–	42
6.5	B	Ti-22Al-27Nb	PM+HR+H	–	1068	1260	2.3		–	–	–	42
7.1	TiB_2	Ti-6Al-4V	RS+HIP	548	–	–	–	130.8	–	–	–	44
7.1	TiB_2	Ti-6Al-4V	RS+H+ HIP+F	550	–	–	–	132.8	–	–	–	44
10	B	Ti-6Al-4V	MA+HIP	–	–	–	0.25	136.6	–	–	–	45
10	B	Ti-4.0Fe-7.3Mo	SPS	–	–	–	–	137	1560	9.57	Density ~99.5%	7
10	B	Ti	VAR (MACS) +HS	–	706	902	5.6	131	–	–	–	43
10	–	Ti-24Al-10Nb (at. %)	PM+HIP	–	–	695	0.0	–	–	–	Specimens failed before yielding	4
10	TiB_2	Ti-6Al-4V	CS+HIP	~550	–	–	–	–	–	–	Ti added to matrix	36
10	CrB	Ti-6Al-4V	CS+HIP	~430	–	–	–	–	–	–	Cr added to matrix	36
10	TiB_2	Ti-4Fe-7.3Mo	MA+SPS	–	–	–	–	146	1007	8.64	Density 99.60%	31
11	TiB_2	Ti-6Al-4V	GA+HIP/ Extrusion		1315	1470	3.1	144	–	–	–	46
15	B	Ti	VAR (MACS) +HS	–	842	903	0.4	139	–	–	–	43
15	–	Ti-5Al-2.5Fe	PM+HIP	–	–	1092	0.0	151	–	–	Specimens failed before yielding	4
15	B	Ti-4.0Fe-7.3Mo	SPS	–	–	–	–	~145	~1053	~8.2	Density ~98.8%	7
15	CrB	Ti-6Al-4V	CS+HIP	~470	–	–	–	–	–	–	Cr added to matrix	36
15	TiB_2	Ti-6Al-4V	CS+HIP	~630	–	–	–		–	–	Ti added to matrix	36
20	TiB_2	Ti	RHP	550	–	–	–	160	–	–	–	2

Table 1 continued

TiB vol. %	Boron Source	Matrix	Process	Properties							Comments	Ref.
				VHN (or HRA)	Yield Strength (MPa)	UTS (MPa)	Ductility %	Young's Modulus (GPa)	Flexural Strength (MPa)	K_{1C} (MPa.m$^{1/2}$)		
20	TiB_2	Ti-6Al-4V	RHP	580	–	–	–	–	–	–	–	2
20	TiB_2	Ti	PM	–	–	673	0.0	148	–	–	–	46
20	TiB_2	Ti-6Al-4V	MA+HIP	–	1170		2.5	154	–	–	–	46
20	B	Ti-4.0Fe-7.3Mo	SPS	–	–	~7.7	–	~160	~905	–	Density ~97.8%	7
20	TiB_2	Ti-6Al-4V	PM+E MA+HP+E	–	1181	1215	0.5	170	–	–	TiB aligned	33
20	TiB_2	Ti-6Al-4V	CS+HIP	~710	–	–	–	–	–	–	Ti added to matrix	36
20	TiB2	Ti-6Al-4V	MA+HP	–	–	1018	0.1	145	–	–	TiB randomly oriented	33
30	B	Ti-4.3Fe-7Mo-1.4Al-1.4V	MA+CIP+ Sintering +Hot swaging	–	–	1700	0.5	160	–	–	–	4
34	B	Ti-6.4Fe-10.3Mo	PM+HP	–	–	736	0.5	163	–	–	Specimens failed before yielding	26
34	B	Ti-24.3Mo	PM+HP+HT	–	–	1105	0.9	171	–	–	Specimens failed before yielding	26
34	B	Ti-53Nb	PM+HP+HT	–	710	724	1.7	122	–	–	Specimens failed before yielding	26
40	TiB_2	Ti-6Al-4V	PM+E MA+HP+E	–	–	864	0.0	210	–	–	TiB aligned	33
~40	B	Ti	SHS/ PHIP	(82.7 HRA)	–	140	–	191.5	193	6.11	Density 94.3%	30
~50	B	Ti	SHS/ PHIP	–	–	224	–	227	449	–	Density >94%	30
54	TiB_2	Ti	RHP	–	–	–	–	210	–	–		21
~60	B	Ti	SHS/ PHIP	(84.3 HRA)	–	280	–	271	515	6.22	Density 97.04%	30
67	TiB_2	Ti	RHP	1351	–	–	–	–	350	–	TiB particles	27
69	TiB_2	Ti	RHP	–	–	–	–	276	–	–	–	21
~70	B	Ti	SHS/PHIP	(87.8 HRA)	–	248.8	–	326	416.4	6.15	Density 98.45%	30
~80	B	Ti	SHS/ PHIP	(86.7 HRA)	–	207	–	391	277	5.23	Density 97.57%	30
83	TiB_2	Ti	RHP		–		–	366	–	–	–	21
100	B	Ti	SHS/PHIP	(87.1 HRA)	–	103	–	550	225	3.36	Density 96.86%	30

PM = Powder Metallurgy Processing, F = Forging, GA = Argon Gas Atomization, MA = Mechanical Alloying, RS = Rapidly Solidified, H = Heat Treated, E = Extrusion, CS = Combustion Synthesis, SHS = Self Propagating High Temperature Synthesis, RHP = Reactive Hot Pressing, HIP = Hot Isostatic Pressing, PHIP = Pseudo Hot Isostatic Pressing, DTA = Differential Thermal Analysis, SPS = Spark Plasma Sintering, HP = hot pressing, HR = hot rolling, YS = Yield Strength, VHN = Vickers Hardness Number, HRA = Rockwell Hardness (scale A), MACS = Melt Assisted Combustion Synthesis, HS = Hot Swaging, VAR = Vacuum Arc Remelting, ~ = Data extracted from plots (in the TiB volume % column it means value is in weight %)

this, covering reported work from 0.039 to 1.0 TiB volume fractions and also incorporating fracture toughness reported data. It must be stated that the compiled data involves a number of Ti matrices of different compositions. While the TiB volume fraction is certainly a contributing factor to the properties

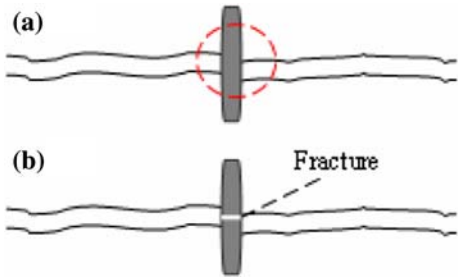

Fig. 6 (**a**) Crack-bridging of TiB and (**b**) Whisker fracture

reported, the TiB aspect ratio, matrix composition and processing history are also expected to be important, and the properties should be observed in light of these contributing factors. For example, the matrix composition whether it is alpha Ti, alpha/Beta Ti or Beta Ti could have a considerable effect on the ductility of the final composite. As previously mentioned, Panda and Ravi Chandran [26] have recently shown this quite effectively through the use of beta Ti stabilizers in Ti–TiB composites. Beta titanium is generally known to be more ductile than alpha Ti with less sensitivity to interstitial impurities. Hence beta Ti stabilization of the Ti matrix can significantly improve the ductility of the Ti–TiB composite. This is certainly true and can be seen from Table 1 for the results at 20 vol.% TiB, where the composite with the pure Ti matrix shows the lowest ductility compared to other matrices with beta stabilizers. However as seen from Table 1, at a number of volume fractions (e.g., 10 and 15 vol.%) pure Ti matrices appear to result in better ductilities than matrices having beta stabilizers. Again here the processing history (and therefore resulting microstructure) of these composites of the same TiB volume % is generally different which is certainly a contributing factor as mentioned previously. In fact this is clearly shown for the 6.5 vol.% TiB reinforced material, where the exact same matrix composition is used but when different processing methods were applied, the ductility changed. Hence as previously mentioned, the compiled results should be viewed in light of the above mentioned contributing factors.

Conclusions

It is clear that the interest in Ti–TiB composites is gaining momentum. The work carried out to date has significantly contributed to our current understanding of the microstructural and morphological development of these in-situ composites. Moreover, the mechanical properties have also been characterized to a good extent; but further work is also needed in this area. In addition, there are still a number of areas that may warrant further research. These include the control of TiB size/size distribution and overcoming the low fracture toughness and ductility at high TiB volume fractions possibly through adopting new strategies for microstructural design.

Acknowledgments The authors would like to thank the San Diego State University Research foundation for sponsoring the initiation of the Ti–TiB research work under the Research Scholarship & Creative Activities, and Faculty Development Program grants.

References

1. Tjong SC, Wang G (2005) Adv Eng Mater 7(1–2):63
2. Gorsse S, Chaminade JP, Petitcorps YL (1998) Composites Part A 29(A):1229
3. Liu G, Zhu D, Shang J-K (1993) Scripta Metall et Mater 28(6):729
4. Ravi Chandran KS, Panda KB, Sahay SS (2004) JOM 56(5):42
5. Ma ZY, Tjong SC, Gen L (2000) Scripta Mater 42:367
6. Zhang E, Jin Y, Wang H, Zeng S (2002) J Mater Sci 37(9):1861
7. Feng H, Zhou Y, Jia D, Meng Q (2004) Comp Sci Tech 64(16):2495
8. Saito T (2004) JOM 56(5):33
9. Abkowitz S, Abkowitz SM, Fisher H, Schwartz PJ (2004) JOM 56(5):37
10. Froes FH, Friedrich H, Kiese J, Bergoint D (2004) JOM 56(2):40
11. Ranganath S (1996) ''Discontinuously reinforced titanium matrix composites via combustion-assisted synthesis in Inorganic matrix composites'', Proceedings of the discussion meeting sponsored by Jawarharal Nehru Center for Advanced Scientific Research and the Structural Materials division of TMS held at the Indian Institute of Science, Bangalore, India, March 8–11,1996 (edited by M.K. Surappa), p. 227
12. Panda KB, Ravi Chandran KS (2003) Metall Mater Trans 34A(9):1993
13. Lu WJ, Zhang D, Wu RJ, Mori H (2002) Metall Mater Trans 33(9):3055
14. Geng K, Lu W, Qin Y, Zhang D (2004) Mater Res Bull 39(6):873
15. Tjong SC, Ma ZY (2000) Mater Sci Eng Rep 29(3):49
16. Morsi K, Moussa SO, Wall J (2005) J Mater Sci 40(4):1027
17. Morsi K, Mcshane H, Mclean M (2000) Metall Mater Trans A 31(6):1663
18. Morsi K, Mcshane H, Mclean M (2000) Mater Sci Eng A 290(1):39
19. Yang YQ, Dudek HJ, Kumudek J (1998) Mater Sci Eng A A246(1–2):213
20. Murray JL (1987) Handbook of binary phase diagrams, 547 pp
21. Atri RR, Ravishandran KS, Jha SK (1999) Mater Sci Eng A A271(1–2):150

22. Fan Z, Miodownik AP, Chandrasekaran L, Ward-Close M (1999) J Mater Sci 29(4):1127
23. Fan Z, Guo ZX, Cantor B (1997) Composites 28(2):131
24. Li BS, Shang JL, Guo JJ, Fu HZ (2004) J Mater Sci 39(3):1131
25. Zhang X, Lu W, Zhang D, Wu R (1999) Scripta Mater 41(1):39
26. Panda KB, Ravi Chandran KS (2003) Metall Mater Trans A 34A(6):1371
27. Radhakrishna Bhat BV, Subramanyam J, Bhanu Prasad VV (2002) Mater Sci Eng A A325(1–2):126
28. Sahay SS, Ravi Chandran KS, Atri R, Chen B, Rubin J (1999) J Mater Res 14(11):4214
29. Feng H-B, Jia D-C, Zhou Y, Hou J (2004) Mater Sci Tech 20(9):1205
30. Xinghong Z, Qiang X, Jiecai H, Kvanin VL (2003) Mater Sci Eng A 348(1–2):41
31. Feng H, Jia D, Zhou Y (2005) Composites Part A 36(5):558
32. Yamamoto T, Otsuki A, Ishihara K, Shingu PH (1997) Mater Sci Eng A A239–240:647
33. Gorsse S, Miracle DM (2003) Acta Mater 51(9):2427
34. Yoshihiro T, Tsuchiyama T, Takaki S (2004) Mater Trans 45(5):1640
35. Morsi K (2001) Mater Sci Eng A A299(1–2):1
36. Kobayashi M, Funami K, Suzuki S, Ouchi C (1998) Mater Sci Eng A A243(1–2):279
37. Banerjee R, Genc A, Hill D, Collins PC, Fraser HL (2005) Scripta Mater 53(12):1433
38. Cullity BD (1978) Elements of X-Ray Diffraction, 2nd edn. Addison-Wesley Pub. Co., p. 391
39. Mallick PK (1988) Fiber-reinforced composites: Materials manufacturing and design. Marcel Dekker, New York, p. 111
40. Fan Z, Miodownik AP, Chandrasekaran L, Ward-Close M (1999) J Mater Sci 29(4):1127
41. Soboyejo WO, Shen W, Srivatsan TS (2004) Mech Mater 36(1–2):141
42. Emura S, Yang SJ, Hagiwara M (2004) Metall Mater Trans A 35A(9):2971
43. Tsang HT, Chao CG, Ma CY (1997) Scripta Mater 37(9):1359
44. Fan Z, Chandrasekaran L, Ward-Close CM, Miodownik AP (1995) Scripta Metall et Mater 32(6):833
45. Godfrey TMT, Wisbey A, Goodwin PS, Bagnall K, Ward-Close CM (2000) Mater Sci Eng A A282(1):240
46. Ravi Chandran KS, Panda KB (2002) Adv Mater Proc 160(10):59
47. Godfrey TMT, Goodwin PS, Ward-Close CM (2000) Adv Eng Mater 2(3):85
48. Saito T, Takamiya H, Furuta T (1998) Mater Sci Eng A A243(1–2):273
49. Li BS, Shang JL, Fu HZ (2004) Mater Sci Eng A A383(2):316